Since January 2020 Elsevier has created a COVID-19 resource centre with free information in English and Mandarin on the novel coronavirus COVID-19. The COVID-19 resource centre is hosted on Elsevier Connect, the company's public news and information website.

Available online at www.sciencedirect.com
ScienceDirect
Biochemical and Biophysical Research Communications 354 (2007) 872–878
BBRC
www.elsevier.com/locate/ybbrc

Discovery of small-molecule HIV-1 fusion and integrase inhibitors oleuropein and hydroxytyrosol: Part I. Integrase inhibition

Sylvia Lee-Huang [a,*,1,2], Philip Lin Huang [b,2,3], Dawei Zhang [a,3], Jae Wook Lee [c], Ju Bao [c], Yongtao Sun [a], Young-Tae Chang [c], John Zhang [c], Paul Lee Huang [d,2]

[a] *Department of Biochemistry, New York University School of Medicine, New York, NY 10016, USA*
[b] *American Biosciences, Boston, MA 02114, USA*
[c] *Department of Chemistry, New York University, New York, NY 10003, USA*
[d] *Department of Medicine, Massachusetts General Hospital and Harvard Medical School, Boston, MA 02114, USA*

Received 4 January 2007
Available online 24 January 2007

Abstract

We have identified oleuropein (Ole) and hydroxytyrosol (HT) as a unique class of HIV-1 inhibitors from olive leaf extracts effective against viral fusion and integration. We used molecular docking simulation to study the interactions of Ole and HT with viral targets. We find that Ole and HT bind to the conserved hydrophobic pocket on the surface of the HIV-gp41 fusion domain by hydrogen bonds with Q577 and hydrophobic interactions with I573, G572, and L568 on the gp41 N-terminal heptad repeat peptide N36, interfering with formation of the gp41 fusion-active core. To test and confirm modeling predications, we examined the effect of Ole and HT on HIV-1 fusion complex formation using native polyacrylamide gel electrophoresis and circular dichroism spectroscopy. Ole and HT exhibit dose-dependent inhibition on HIV-1 fusion core formation with EC_{50}s of 66–58 nM, with no detectable toxicity. Our findings on effects of HIV-1 integrase are reported in the subsequent article.

Keywords: HIV-1; AIDS; Natural product; Small-molecule HIV-1 inhibitors; HIV-1 entry inhibitor; Olive leaf extract (OLE); Oleuropein (Ole); Hydroxytyrosol (HT); Structure–function; Molecular modeling

At present, 29 drugs are licensed by the FDA for the treatment of HIV-1 infection in the United States [1]. These agents can be classified according to their mechanism of action: reverse transcriptase inhibitors (RTIs) (nucleoside, NRTIs and non-nucleoside, NNRTIs), protease inhibitors (PIs), fusion inhibitors, and multi-class combination products (MCCP). The combination of RTIs and PIs, commonly known as Highly Active Antiretroviral Therapy (HAART) [1,2], has significantly reduced morbidity and mortality, transforming HIV/AIDS into a manageable chronic illness. Although HAART can favorably influence disease progression, it does not cure HIV infection. Antiviral therapy must be maintained long-term, and serious chronic toxicity, therapy fatigue, and drug resistance have become major issues.

New therapeutic approaches include the fusion inhibitor Fuzeon (T-20, enfuvirtide), the non-peptidic PI Tipranavir, the new PI darunavir and the recently approved MCCP Atripla. However, existing experience with HIV-1 highlights the need to use multiple effective agents in combination for maximal and durable effect. Thus, the search for novel anti-HIV agents continues to be of great significance, especially those capable of affecting multiple stages of the viral life cycle.

We previously reported that olive leaf extract is potent against HIV-1 [3]. We investigated its anti-HIV properties

* Corresponding author. Fax: +1 212 263 8166.
E-mail address: sylvia.lee-huang@med.nyu.edu (S. Lee-Huang).
[1] Supported by PHS Grant R01-AT01383 to S.L.H.
[2] This paper is dedicated to the memory of Mrs. An Fu Lee, devoted and beloved mother and grandmother.
[3] These authors contributed equally to this work.

0006-291X/$ - see front matter © 2007 Elsevier Inc. All rights reserved.
doi:10.1016/j.bbrc.2007.01.071

and discovered that oleuropein (Ole) and its main metabolite, hydroxytyrosol (HT) are the key anti-HIV components. They are active against multiple stages of the HIV-1 life cycle, inhibiting cell-to-cell HIV-1 transmission and viral core antigen p24 production. Molecular docking simulations indicate that Ole and HT interact with the conserved hydrophobic pocket on the surface of the central trimeric coiled-coil of HIV-gp41 fusion complex, the six helical bundle (6HB), and the catalytic core domain (CCD) of HIV-1 integrase active site. In this article, we report our findings on identification and characterization of Ole and HT, as well as testing and confirmation of modeling predictions on their anti-HIV fusion activity.

Materials and methods

Oleuropein (Ole) and hydroxytyrosol (HT). Oleuropein (Ole) was purified from olive leaf extract, characterized, and standardized by liquid chromatography–coupled mass spectrometry (LC–MS) [3]. Hydroxytyrosol (HT) was prepared by stepwise hydrolysis of Ole with β-glucosidase (Sigma G4511) in 80 mM sodium acetate, pH 5.0 using 1 U/μmole substrate at 37 °C for 1 h. This treatment removes the glucose moiety from Ole and yields oleuropein aglycone (Ole-AG). Ole-AG was subsequently hydrolyzed with esterase (Sigma E0887) in 50 mM sodium phosphate buffer at pH 7.5 at 1 U/μmole substrate at 25 °C for 1 h to yield hydroxytyrosol and elenolic acid. The mixture was separated by HPLC and standardized by LC–MS. HT was also prepared by chemical synthesis from 3,4-dihydroxylphenylacetic ester (DHPA).

Cell lines and HIV-1. Uninfected MT2 and H9 cell lines, and HIV-1_{IIIB} chronically infected H9 (H9/HIV-1_{IIIB}) and HIV-1/IIIB virus, were obtained through the AIDS Research and Reference Reagent Program, NIAID, NIH. MT2 cells [4,5] were obtained from Richman, and H9 and HIV-1IIIB virus stocks [6,7] from Gallo. The cell lines were cultured in RPMI medium 1640 containing 100 U/ml penicillin, 100 μg/ml streptomycin, 2 mM L-glutamine, and 10% heat-inactivated fetal calf serum. Viral stocks were prepared and standardized as described [8].

Anti-HIV and cytotoxicity assays. The effects of Ole and HT on acute HIV infection and viral replication were measured by assays on syncytial formation in cell–cell HIV-1 transmission and on HIV-1 core protein p24 expression as described [8]. Cytotoxicity was evaluated by the MTT assay [8].

Molecular modeling. Molecular modeling was performed by molecular docking, molecular dynamics (MD) simulation, and free energy calculations [9,10]. Docking was performed with Autodock version 3.0.5 [11]. The relaxation of docking structure obtained was then implemented under Discovery from Insight II (Accelrys Inc., San Diego, CA, USA) using 500 steps of Steepest Descent followed by Conjugate Gradient until the root mean square of the energy gradient reaches a value of 0.01 kcal/mol Å.

HIV-1 gp41 fusion peptides C34 and N36. HIV-1 gp41 fusion peptides, N36 and C34 were synthesized by solid-phase FMOC method (GeneMed, CA) and purified by HPLC. The sequences of these peptides are (Ac-SGIVQQQNNLLRAIEAQQHLLQLTVWGIKQLQARIL-NH_2) and (Ac-WMEWDREINNYTSLIHSLIEESQNQQEKNEQELL-NH_2), respectively. Corresponding viral peptides N36 and C34 prepared from HIV-1 were obtained through the NIH AIDS Research and Reference Reagent Program, NIAID, NIH [12] and used as standards for purification and bioassays.

Fusion complex formation. Fusion complex formation was carried out by incubating equimolar amounts of HIV-1 gp41 fusion peptides N36 and C34 in PBS (phosphate-buffered saline, containing 50 mM sodium phosphate, pH 7.2 and 150 mM NaCl) at 10 or 20 μM each at 37 °C. Peptide N36 was first incubated either alone or with various concentrations of Ole or HT for 30 min. Next, an equimolar amount of C34 was added and the samples incubated for 30 min.

Native polyacrylamide gel electrophoresis (N-PAGE). N-PAGE was carried out as previously reported [13] with modifications that involve fusion peptide concentration, order of reactions, and time of incubation in fusion complex formation. Tris-glycine gels (18%, Invitrogen, Carlsbad, CA) were electrophoresed at 120 V for 2 h, stained with Coomassie blue and analyzed by densitometry.

Circular dichroism (CD) spectroscopy. CD spectra were recorded on an AVIV 62-DS CD spectrometer, using 1 mm sample cells and a fixed temperature of 4 °C [8]. Each spectrum is a smoothed average of 10 scans. The bandwidth for each measurement was 1 nm. CD intensities are expressed as mean residue ellipticities [θ] (degrees cm^2/dmol). Prior to calculation of the final ellipticity, all spectra were corrected by subtracting the reference spectra of PBS without peptides.

Results

Preparation and LC–MS analysis of oleuropein (Ole) and hydroxytyrosol (HT)

Fig. 1A–D represent LC–MS analysis of Ole and HT. Ole fractionates as a single peak by HPLC at 1.848 min with *m/z* of 539 and HT as a single peak by HPLC at 1.108 min with *m/z* of 153. Fig. 1E shows the major steps in Ole metabolism. These are also the basic reactions in HT preparation from Ole. First, the glucose moiety is removed by β-glycosidase to yield oleuropein aglycone (Ole–AG). Next, Ole–AG is hydrolyzed by esterase to yield HT and elenolic acid (EA). Fig. 1F shows chemical synthesis of HT using 3,4-dihydroxylphenylacetic acid (DHPAA) as the starting material. Two major steps are involved: (1) acetylation with acetyl chloride (AcCl), and (2) reduction by $LiAlH_4$ to yield HT. Chemically synthesized HT was purified and characterized by LC–MS, and demonstrates identical biological, chemical and physical properties as natural HT prepared from Ole from olive leaf extract.

Ole and HT inhibit HIV-1 infection and replication, but are not toxic to target cells

Ole and HT exhibit dose-dependent inhibition of HIV-1 infection and replication as measured by syncytial formation and p24 production (Table 1). The average EC_{50} for Ole is 55 nM for syncytial formation and 73 nM for p24 production. The corresponding EC_{50}s are 61 and 68 nM for HT. No cytotoxicity was detected, either by MTT assay or trypan blue dye exclusion, over a 10,000-fold concentration range from 1 nM to 10 μM. The EC_{50}s for inhibition on fusion complex, 6HB formation are also presented in Table 1.

Ole and HT bind to the conserved hydrophobic pocket on the surface of the central trimeric coiled-coil of HIV-1 gp41

Inhibition of syncytial formation by Ole and HT reflects effects on early events during viral infection/entry, including CD4 receptor and coreceptor binding as well as viral fusion. To probe anti-HIV mechanisms of Ole and HT, we carried out molecular docking and MD calculations of these small molecules with viral targets. We found that

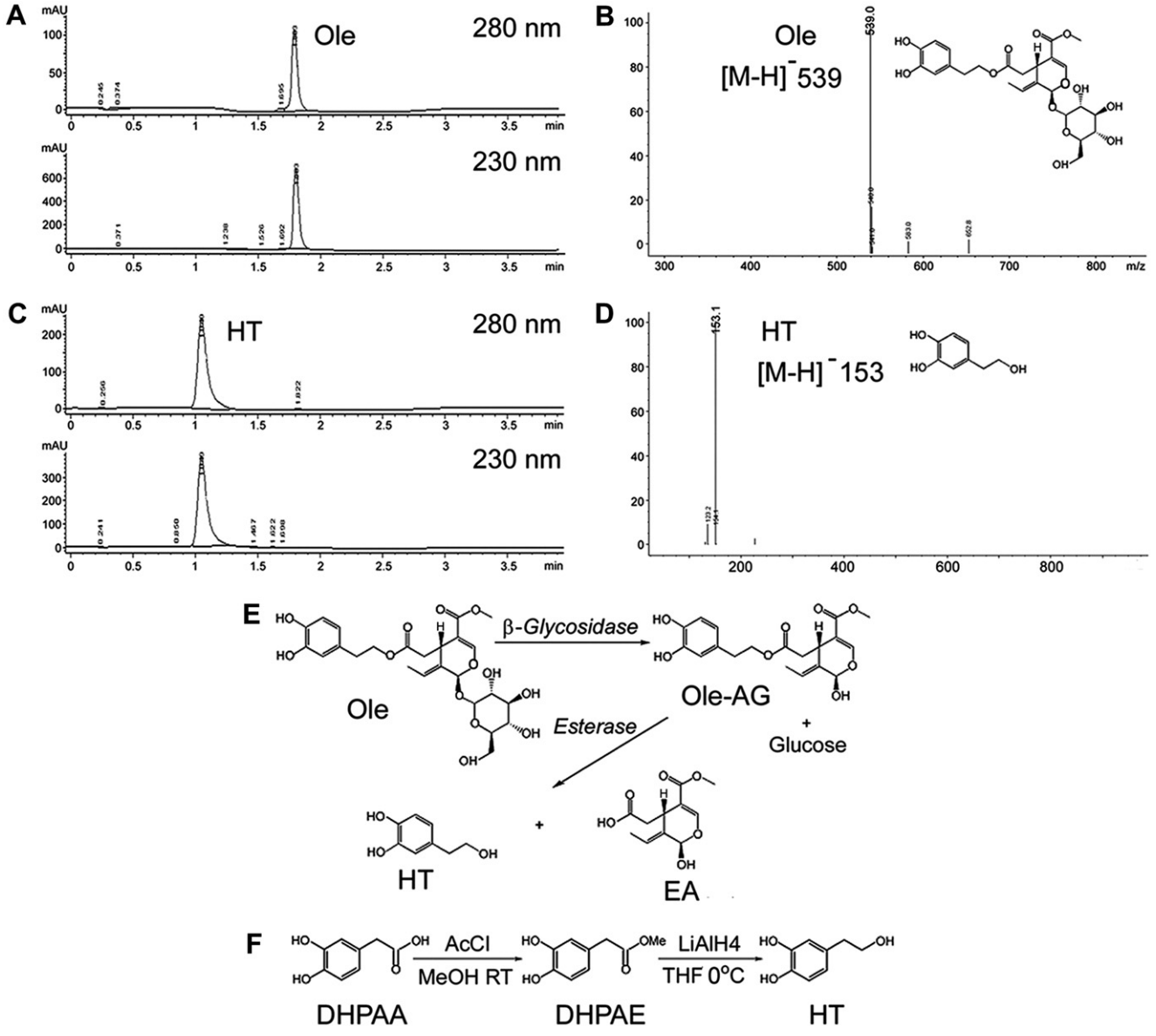

Fig. 1. LC–MS analysis of Ole and HT, metabolism of Ole and chemical synthesis of HT. (A) LC elution profile of Ole. (B) MS analysis of Ole, showing one major component with a molecular mass of 539. (C) LC elution profile of HT. (D) MS analysis of HT, showing one major component with a molecular mass of 153. (E) Metabolism of Ole, showing major reactions in the production of HT from Ole. (F) Chemical synthesis of HT.

Table 1
Anti-HIV activity and inhibition on HIV-1 fusion core formation

Compound	Anti-HIV activity[a]			Inhibitory activity[b] EC_{50} (nM)	
	EC_{50} (nM)		IC_{50} (nM)	Fusion core formation 6HB (N36+C34)	
	Syncytium	P24	Cytotoxicity	N-PAGE	CDSA
Ole	55 ± 5	73 ± 8	>10,000	66 ± 5	62 ± 6
HT	61 ± 6	68 ± 8	>10,000	58 ± 8	60 ± 4

[a] EC_{50}, effective concentration at 50% inhibition; IC_{50}, cytotoxicity concentration at 50% inhibition.
[b] N-PAGE, native polyacrylamide gel electrophoresis; CDSA, circular dichroism spectroscopy analysis. Values are means ± SD of triplicates in three independent determinations.

Ole and HT bind to the conserved hydrophobic pocket on the surface of the central trimeric coiled-coil of the HIV-1 gp41 fusion domain.

HIV-1 envelope glycoprotein (Env) mediates viral entry by fusing virus to target cells. Env is trimeric on the virion surface. Each monomer contains a surface subunit, gp120,

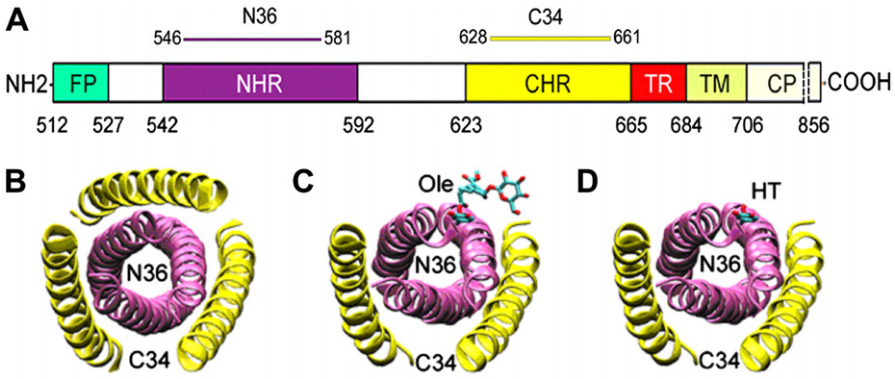

Fig. 2. HIV-1 gp41 and the formation of fusion core 6HB. (A) Structure map of HIV-1 gp41, FP (fusion peptide), NHR (N-terminal heptad repeat), CHR (C-terminal heptad repeat), TR (tryptophan-rich), TM (transmembrane), and CP (cytoplasmic) domains. Residue numbers correspond to positions in gp160 of HIV-1HXB2. (B) Formation of 6HB by N36 and C34 helices, showing the trimeric coiled-coil core of N36 and the surrounding three C34s. (C,D) Effect of Ole and HT on fusion core, 6HB formation, showing the binding of Ole or HT to the N36 trimeric coiled-coil core thus inhibiting 6HB formation.

for virus binding to CD4 receptor and coreceptors [14–17] and a noncovalently associated transmembrane subunit, gp41, that mediates fusion of the virus with the target cell [18,19]. Fig. 2A shows the structure of HIV-1 gp41. Like other type I transmembrane proteins, HIV-1 gp41 consists of extracellular (ectodomain), transmembrane, and cytoplasmic domains. The ectodomain contains four functional regions: the fusion peptide (FP), N-terminal heptad repeat (NHR), C-terminal heptad repeat (CHR), and a tryptophan-rich region (TR). Binding of gp120 to the cellular receptor CD4 and coreceptor triggers conformational changes in gp41 that induce fusion [20–23]. This increases exposure of two heptad repeat motifs, NHR and CHR, and insertion of the fusion peptide into the target membrane [20–23]. Subsequently NHR and CHR fold in an antiparallel manner to create the six-helix bundle 6HB composed of a trimeric NHR coiled-coil core surrounded by three CHR helices that pack in the grooves of the coiled-coil as seen in Fig. 2B [24–26]. Formation of the 6HB promotes fusion between viral and cellular membranes and is essential for viral entry and infection [25,26]. Ole and HT interact with the NHR coiled-coil trimer N36 helices

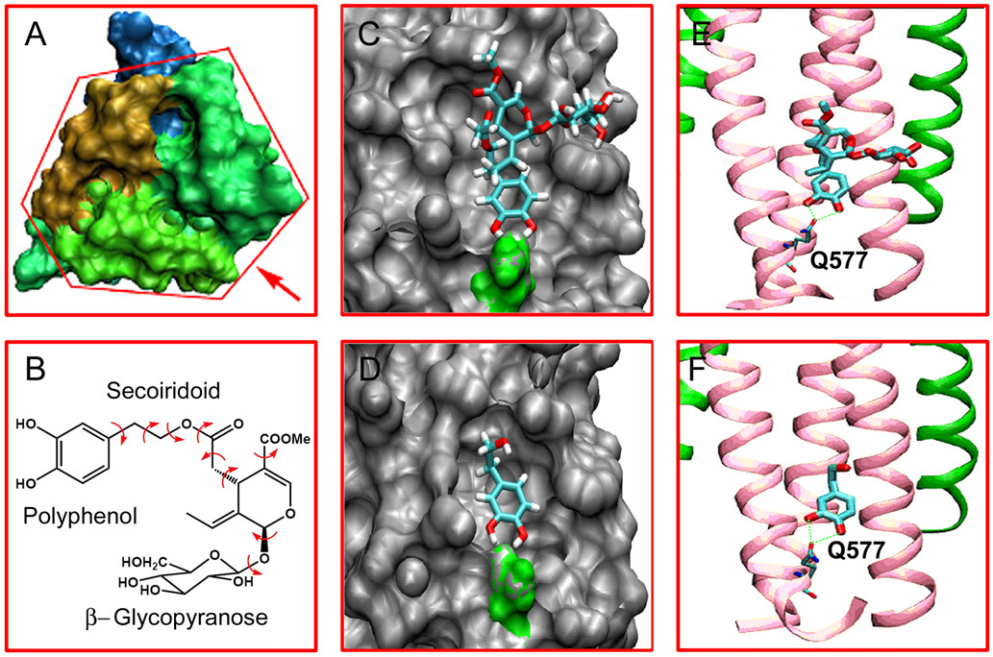

Fig. 3. Molecular docking of Ole and HT with HIV-1 gp41. (A) Structures of the 5-helical gp41 bundle. (B) Structure of Ole. The nine freely rotating bonds are shown. (C,D) The predicted binding structures of Ole (C) and HT (D) inside the HIV-1 gp41 hydrophobic site. gp41 is shown as a surface model and Ole and HT are shown as stick models. Both molecules form stable hydrogen bonds with Q577 (green) on N36 peptide. (E,F) Ribbon representation showing hydrogen binding of gp41 5HB with Ole (E) and HT (F). The trimeric coiled-coil core of N36 peptides are pink and C34 peptides green. The Ole and HT molecules are shown as stick formation and hydrogen bonds with Q577 are in green dashed lines.

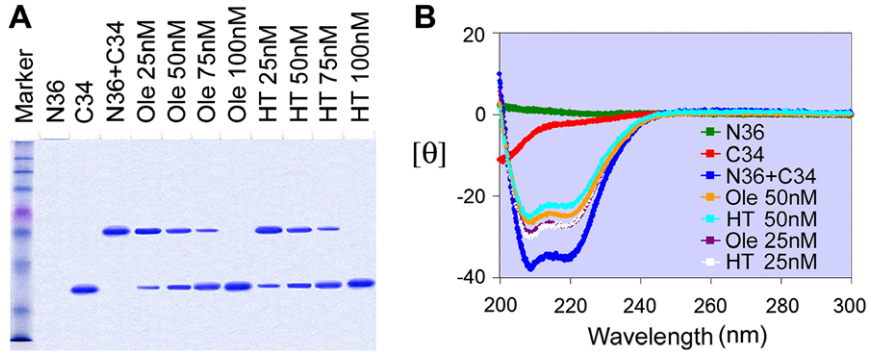

Fig. 4. The effect of Ole and HT on the formation of 6HB between HIV-1 peptides N36 and C34. (A) Native PAGE was carried out in Tris-glycine 18% gels, at 120 V constant voltages at room temperature for 2 h. The gel was then stained with Coomassie blue and analyzed by densitometry. Lane 1, molecular weight markers; lane 2, N36; lane 3, C34; lane 4 fusion complex, (N36 + C34); lanes 5–8 and 9–12, in the presence of Ole and HT at 25, 50, 75, and 100 nM. (B) CD analysis, CD spectra for N36 (green), C34 (red), (N36 + C34) 6HB (blue), and N36 + C34 in the presence of 25 and 50 nM of Ole or HT.

and interfere with the formation of 6HB with the CHR, C34, as shown in Fig. 2C and D.

We used the crystal structure of the HIV-1 gp41 fusion complex, PDB code 1AIK [20] as a reference for our modeling work. To provide a ligand-binding site, one of the C34 helices was removed from the 6HB (Fig. 3A). Fig. 3B shows the chemical structure of Ole with the 9 free rotatable bonds selected in our modeling interaction.

Molecular simulations suggest that the conserved hydrophobic cavity of the gp41 N36 trimer coiled-coil is the most likely binding site for Ole and HT. This cavity is mainly occupied by W628, W631, and neighboring I635 and D632. The predicted binding structures of Ole and HT are shown in Fig. 3C and D, respectively. Ole and HT form stable hydrogen bonds with Q577 on the N36 peptide. Fig. 3E and F are ribbon representations of the predicted binding site of Ole and HT. 5HB, consisting of three N36-peptides (pink, residues 546–581) and two C34 peptides (green, residues 628–661), is used for docking calculations. Only one groove is exposed for the binding of small molecules. Both Ole and HT occupy the binding site similarly, with the diphenol ring forming stable hydrogen bonds with Q577. This blocks the close contacts between the hydrophobic groove in the gp41 NHR and the indole rings of W631 and W628, thus interfering with the formation of 6HB. In addition to hydrogen binding, hydrophobic interactions with I573, G572, and L568 also play important roles in the interaction.

Native PAGE shows that Ole and HT inhibit HIV-1 fusion core 6HB formation

To test the predictions from molecular modeling, we examined the effect of Ole and HT on the formation of fusion complex 6HB by electrophoretic mobility shift using native PAGE (Fig. 4A). The electrodes were connected from cathode (negative terminal on top) to anode (positive terminal on bottom) and the peptides move in the electric field according to their charge and size. Peptides carrying net negative charges, such as C34, move toward the positive terminal (bottom) whereas peptides carrying net positive charges, such as N36, move toward the negative terminal or remain at the top of the well. Incubation of N36 and C34 resulted in the formation of the 6HB fusion complex which is larger than C34, moves slower than free C34, and thus migrates to the middle of the gel. Pre-incubation of N36 with Ole or HT results in inhibition of 6HB formation. A dose dependent disappearance of 6HB band was detected with concomitant appearance of the free C34 band. Total inhibition is achieved at 100 nM Ole or HT with EC_{50}s around 66 and 58 nM. These results confirm the predictions from molecular modeling.

CD analysis indicates that Ole and HT inhibit HIV-1 fusion core 6HB formation

We also used CD analysis to confirm molecular modeling predictions (Fig. 4B). Because N36 and C34 are single-stranded random coils, they do not assume ordered structure in solution, so they display characteristic random coil CD spectra. However, formation of fusion complex 6HB results in a distinctive CD spectrum, including a saddle-shaped negative peak between 210 and 220 nm in the far UV region and a significant increase in molar ellipticity (θ) at 222 nm. Pre-incubation of N36 with Ole or HT interrupts 6HB formation and results in a dose-dependent shift of the CD spectra from helical to random coil with EC_{50}s of 62 nM for Ole and 60 nM for HT.

Discussion

Ole and HT are small molecules with molecular weights of 539 and 153, respectively. Their inhibition of the fusion-promoting refolding of gp41 is an excellent example of how small molecules can block formation of protein–protein complexes. We narrowed down the target of binding to a hydrophobic pocket on the gp41 inner core. This pocket is highly conserved among the different HIV clades.

Consistent with this, we found that Ole and HT are active against a panel of HIV-1 primary isolates that includes both M and T tropic strains from different clades. Our results suggest that Ole and HT may be useful against other viruses with type I transmembrane envelope glycoprotein, including severe acute respiratory syndrome associated coronavirus [23,27], respiratory syncytial virus, Ebola virus [28], measles virus [29], and avian flu virus [30,31].

Fuzeon (T-20 or Enfuvirtide) is the only FDA approved HIV fusion inhibitor [32,33]. It is a peptide derived from the CHR region of gp41 that partially overlaps with the C34 sequence. Fuzeon is commercially produced by chemical synthesis. Because of its large size—it consists of 36 amino acids with a molecular weight of 4492—its manufacturing process is very complex, involving 106 chemical steps [34,35]. In contrast, our typical process for chemical synthesis of HT involves only two steps: acetylation and reduction (Fig. 1F). In addition, Ole and HT can also be easily prepared from natural olive leaf extract in only two steps: deglycosylation and oxidation (Fig. 1E). The fact that Ole and HT act both outside and inside of the cellular environments in viral entry and integration offers unique benefits to these small molecules against viral resistance.

Acknowledgments

This work was supported in part by Public Health Service Grant R01 AT01383, NCCAM, NIH to S.L.H. We are grateful to Dr. Helen C. Lin for support and encouragement.

References

[1] S.M. Hammer, Clinical practice. Management of newly diagnosed HIV infection, N. Engl. J. Med. 353 (2005) 1702–1710.
[2] J. Cohen, Therapies. Confronting the limits of success, Science 296 (2002) 2320–2324.
[3] S. Lee-Huang, L. Zhang, P.L. Huang, Y.T. Chang, Anti-HIV activity of olive leaf extract (OLE) and modulation of host cell gene expression by HIV-1 infection and OLE treatment, Biochem. Biophys. Res. Commun. 307 (2003) 1029–1037.
[4] T. Haertle, C.J. Carrera, D.B. Wasson, L.C. Sowers, D.D. Richman, D.A. Carson, Metabolism and anti-human immunodeficiency virus-1 activity of 2-halo-2′,3′-dideoxyadenosine derivatives, J. Biol. Chem. 263 (1988) 5870–5875.
[5] S. Harada, Y. Koyanagi, N. Yamamoto, Infection of HTLV-III/LAV in HTLV-I-carrying cells MT-2 and MT-4 and application in a plaque assay, Science 229 (1985) 563–566.
[6] D.L. Mann, S.J. O'Brien, D.A. Gilbert, Y. Reid, M. Popovic, E. Read-Connole, R.C. Gallo, A.F. Gazdar, Origin of the HIV-susceptible human CD4+ cell line H9, AIDS Res. Hum. Retroviruses 5 (1989) 253–255.
[7] M. Popovic, M.G. Sarngadharan, E. Read, R.C. Gallo, Detection, isolation, and continuous production of cytopathic retroviruses (HTLV-III) from patients with AIDS and pre-AIDS, Science 224 (1984) 497–500.
[8] S. Lee-Huang, V. Maiorov, P.L. Huang, A. Ng, H.C. Lee, Y.T. Chang, N. Kallenbach, P.L. Huang, H.C. Chen, Structural and functional modeling of human lysozyme reveals a unique nonapeptide, HL9, with anti-HIV activity, Biochemistry 44 (2005) 4648–4655.
[9] D.A. Case, T.E. Cheatham 3rd, T. Darden, H. Gohlke, R. Luo, K.M. Merz Jr., A. Onufriev, C. Simmerling, B. Wang, R.J. Woods, The Amber biomolecular simulation programs, J. Comput. Chem. 26 (2005) 1668–1688.
[10] Y. Duan, C. Wu, S. Chowdhury, M.C. Lee, G. Xiong, W. Zhang, R. Yang, P. Cieplak, R. Luo, T. Lee, J. Caldwell, J. Wang, P. Kollman, A point-charge force field for molecular mechanics simulations of proteins based on condensed-phase quantum mechanical calculations, J. Comput. Chem. 24 (2003) 1999–2012.
[11] D.S. Goodsell, G.M. Morris, A.J. Olson, Automated docking of flexible ligands: applications of AutoDock, J. Mol. Recognit. 9 (1996) 1–5.
[12] S.A. Gallo, K. Sackett, S.S. Rawat, Y. Shai, R. Blumenthal, The stability of the intact envelope glycoproteins is a major determinant of sensitivity of HIV/SIV to peptidic fusion inhibitors, J. Mol. Biol. 340 (2004) 9–14.
[13] S. Liu, Q. Zhao, S. Jiang, Determination of the HIV-1 gp41 fusogenic core conformation modeled by synthetic peptides: applicable for identification of HIV-1 fusion inhibitors, Peptides 24 (2003) 1303–1313.
[14] Y. Feng, C.C. Broder, P.E. Kennedy, E.A. Berger, HIV-1 entry cofactor: functional cDNA cloning of a seven-transmembrane, G protein-coupled receptor, Science 272 (1996) 872–877.
[15] P.D. Kwong, R. Wyatt, J. Robinson, R.W. Sweet, J. Sodroski, W.A. Hendrickson, Structure of an HIV gp120 envelope glycoprotein in complex with the CD4 receptor and a neutralizing human antibody, Nature 393 (1998) 648–659.
[16] C.D. Rizzuto, R. Wyatt, N. Hernandez-Ramos, Y. Sun, P.D. Kwong, W.A. Hendrickson, J. Sodroski, A conserved HIV gp120 glycoprotein structure involved in chemokine receptor binding, Science 280 (1998) 1949–1953.
[17] Q.J. Sattentau, A.G. Dalgleish, R.A. Weiss, P.C. Beverley, Epitopes of the CD4 antigen and HIV infection, Science 234 (1986) 1120–1123.
[18] D.C. Chan, P.S. Kim, HIV entry and its inhibition, Cell 93 (1998) 681–684.
[19] J. Moore, B. Jameson, R. Weiss, Q. Sattentau, in: J. Benz (Ed.), Viral Fusion Mechanisms, CRC Press, Boca Raton, FL, 1993, pp. 233–289.
[20] D.C. Chan, D. Fass, J.M. Berger, P.S. Kim, Core structure of gp41 from the HIV envelope glycoprotein, Cell 89 (1997) 263–273.
[21] D.M. Eckert, P.S. Kim, Mechanisms of viral membrane fusion and its inhibition, Annu. Rev. Biochem. 70 (2001) 777–810.
[22] M. Lu, S.C. Blacklow, P.S. Kim, A trimeric structural domain of the HIV-1 transmembrane glycoprotein, Nat. Struct. Biol. 2 (1995) 1075–1082.
[23] Y. Xu, Z. Lou, Y. Liu, H. Pang, P. Tien, G.F. Gao, Z. Rao, Crystal structure of severe acute respiratory syndrome coronavirus spike protein fusion core, J. Biol. Chem. 279 (2004) 49414–49419.
[24] S. Jiang, K. Lin, N. Strick, A.R. Neurath, HIV-1 inhibition by a peptide, Nature 365 (1993) 113.
[25] K. Tan, J. Liu, J. Wang, S. Shen, M. Lu, Atomic structure of a thermostable subdomain of HIV-1 gp41, Proc. Natl. Acad. Sci. USA 94 (1997) 12303–12308.
[26] W. Weissenhorn, A. Dessen, S.C. Harrison, J.J. Skehel, D.C. Wiley, Atomic structure of the ectodomain from HIV-1 gp41, Nature 387 (1997) 426–430.
[27] B. Tripet, M.W. Howard, M. Jobling, R.K. Holmes, K.V. Holmes, R.S. Hodges, Structural characterization of the SARS-coronavirus spike S fusion protein core, J. Biol. Chem. 279 (2004) 20836–20849.
[28] W. Weissenhorn, A. Carfi, K.H. Lee, J.J. Skehel, D.C. Wiley, Crystal structure of the Ebola virus membrane fusion subunit, GP2, from the envelope glycoprotein ectodomain, Mol. Cell 2 (1998) 605–616.
[29] D.M. Lambert, S. Barney, A.L. Lambert, K. Guthrie, R. Medinas, D.E. Davis, T. Bucy, J. Erickson, G. Merutka, S.R. Petteway Jr., Peptides from conserved regions of paramyxovirus fusion (F) proteins are potent inhibitors of viral fusion, Proc. Natl. Acad. Sci. USA 93 (1996) 2186–2191.
[30] D. Normile, Avian influenza. New H5N1 strain emerges in southern China, Science 314 (2006) 742.

[31] D.Q. Wei, Q.S. Du, H. Sun, K.C. Chou, Insights from modeling the 3D structure of H5N1 influenza virus neuraminidase and its binding interactions with ligands, Biochem. Biophys. Res. Commun. 344 (2006) 1048–1055.
[32] V. Oldfield, G.M. Keating, G. Plosker, Enfuvirtide: a review of its use in the management of HIV infection, Drugs 65 (2005) 1139–1160.
[33] D. Robertson, US FDA approves new class of HIV therapeutics, Nat. Biotechnol. 21 (2003) 470–471.
[34] B.L. Bray, Large-scale manufacture of peptide therapeutics by chemical synthesis, Nat. Rev. Drug Discov. 2 (2003) 587–593.
[35] A. Castagna, P. Biswas, A. Beretta, A. Lazzarin, The appealing story of HIV entry inhibitors: from discovery of biological mechanisms to drug development, Drugs 65 (2005) 879–904.

Update

Biochemical and Biophysical Research Communications
Volume 356, Issue 4, 18 May 2007, Page 1068

DOI: https://doi.org/10.1016/j.bbrc.2007.03.022

Available online at www.sciencedirect.com
ScienceDirect
Biochemical and Biophysical Research Communications 356 (2007) 1068
BBRC
www.elsevier.com/locate/ybbrc

Erratum

Erratum to "Discovery of small-molecule HIV-1 fusion and integrase inhibitors oleuropein and hydroxytyrosol: Part I. Integrase inhibition" [Biochem. Biophys. Res. Commun. 354 (2007) 872–878]

Sylvia Lee-Huang [a,*], Philip Lin Huang [b], Dawei Zhang [a], Jae Wook Lee [c], Ju Bao [c], Yongtao Sun [a], Young-Tae Chang [c], John Zhang [c], Paul Lee Huang [d]

[a] *Department of Biochemistry, New York University School of Medicine, New York, NY 1006, USA*
[b] *American Biosciences, Boston, MA 02114, USA*
[c] *Department of Chemistry, New York University, New York, NY 10003, USA*
[d] *Department of Medicine, Massachusetts General Hospital and Harvard Medical School, Boston, MA 02114, USA*

Available online 9 March 2007

The publisher regrets that a typesetting error resulted in Parts I and II of this study carrying the same subtitle. The entire title of the article referenced above should read "Discovery of small-molecule HIV-1 fusion and integrase inhibitors oleuropein and hydroxytyrosol: Part I. Fusion inhibition."

DOI of original article: 10.1016/j.bbrc.2007.01.071.
* Corresponding author. Fax: +1 212 263 8166.
E-mail address: sylvia.lee-huang@med.nyu.edu (S. Lee-Huang).

0006-291X/$ - see front matter
doi:10.1016/j.bbrc.2007.03.022